

# Did the Crab Pulsar Undergo a Small Glitch in 2006 late March/early April?

M. Vivekanand<sup>1</sup>

viv.maddali@gmail.com

Received \_\_\_\_\_; accepted \_\_\_\_\_

---

<sup>1</sup>No. 24, NTI Layout 1<sup>st</sup> Stage, 3<sup>rd</sup> Main, 1<sup>st</sup> Cross, Nagasettyhalli, Bangalore 560094, India.

## ABSTRACT

On 2006 August 23 the Crab Pulsar underwent a glitch, that was reported by the Jodrell Bank and the Xinjiang radio observatories. Neither data are available to the public. However, the Jodrell group publishes monthly arrival times of the Crab Pulsar pulse (their actual observations are done daily), using which it is shown that about five months earlier, the Crab Pulsar most probably underwent a small glitch, which has not been reported before. Neither observatory discusses the detailed analysis of data from 2006 March to August; either they may not have detected this small glitch, or may have attributed it to timing noise in the Crab Pulsar. The above result is verified using X-ray data from the RXTE observatory. If this is indeed true, this may probably be the smallest glitch observed in the Crab Pulsar so far, whose implications are discussed. This work addresses the confusion possible between small magnitude glitches and timing noise in pulsars.

*Subject headings:* pulsars: individual (Crab Pulsar) X-rays: stars

## 1. Introduction

Glitches in pulsars are probably the only method of studying the internal structure of neutron stars (Baym et al. (1969), Ruderman et al. (1998)); see Shemar & Lyne (1996) and Lyne et al. (2000) for an observational perspective, and Haskell & Melatos (2015) for a theoretical discussion of pulsar glitches. Among pulsars that have been observed for their glitch behavior, the Crab Pulsar (PSR B0531+21 or J0534+2200) has been the most closely studied (Lyne et al. 2015). Glitches in this pulsar occur, in average, once in 1.5 years. Its several glitches have been analyzed and results for them published by Lyne et al. (1988), Lyne et al. (1993), Lyne et al. (2000), Wong et al. (2001), Espinoza et al. (2011) and Wang et al. (2012), the most recent study being that of Lyne et al. (2015). This work focuses on the glitch that occurred in the Crab Pulsar on 2006 August 23 (henceforth CPG2006); more precisely, on the five month duration before CPG2006. Two radio observatories observed it in sufficient detail to derive the relevant glitch parameters — The Jodrell Bank Observatory (Espinoza et al. (2011); henceforth JBO) and the Xinjiang Astronomical Observatory (Wang et al. (2012); henceforth XAO).

The critical pre-glitch reference timing model is obtained by both groups by fitting a simple rotation model to the timing data for a given duration before the glitch (the pre-glitch duration); the model typically consists of the pulsar rotation frequency  $\nu$  and its first two derivatives  $\dot{\nu}$  and  $\ddot{\nu}$ , at the epoch of the glitch, which is MJD  $\approx 53970$  for both observatories. The pre-glitch duration for the JBO group is about 43 days starting from MJD 53926 (C. Espinoza, private communication), while that of the XAO group is 280 days, from MJD 53685 to MJD 53965. The timing residuals for CPG2006 relative to the pre-glitch reference timing model are analyzed by both groups, obtaining consistent results.

This work shows that a different choice of the pre-glitch duration for CPG2006 reveals what appears to be a small glitch about five months before the main glitch. The monthly

radio timing data of the Crab Pulsar from JBO are used to derive the result, and X-ray data from the RXTE Observatory are used to verify it. In the last section it is argued that this is more likely to be a glitch than timing noise, although the data available strictly do not allow to discriminate between the two possibilities.

## 2. Observations

The Crab Pulsar was monitored daily by JBO since 1984, mainly at 610 MHz frequency (Lyne et al. 2015). Occasionally it was also observed in the 1400 to 1700 MHz band. The XAO has been monitoring the Crab Pulsar once a week at 1540 MHz since 2000 January (Wang et al. 2012). Both groups estimate the arrival time of the integrated pulse profile (IP) of the Crab Pulsar, and use this data to study the several glitches in this pulsar by means of standard techniques. Neither of the above two data are available in the public domain. However JBO also publishes monthly arrival times of the Crab pulsar IP, referred to the Solar System Barycenter, and scaled to infinite frequency, in the so called Jodrell Bank Crab Pulsar Monthly Ephemeris<sup>1</sup> (Lyne et al. (1993); henceforth JBCPME). Data from this ephemeris spanning the epoch 2005 November 15 to 2007 May 15 (MJD 53689 to MJD 54235), yielding 19 timing residuals, have been used for this work. In practice, one requires daily timing residuals to properly analyze the glitches in the Crab Pulsar. However, JBCPME also contains very accurate  $\nu$  and  $\dot{\nu}$  at each monthly epoch, which help in converging to a sufficiently accurate pre-glitch reference timing model. Thus the monthly radio data used in this work are suitable to demonstrate the existence of the smaller glitch, which is the main goal of this work; derivation of statistically rigorous glitch parameters requires the original daily observed data. Although this work uses only the Crab Pulsar’s

---

<sup>1</sup><http://www.jb.man.ac.uk/pulsar/crab.html>

timing residuals, the main result is also evident in the  $\nu$  and  $\dot{\nu}$  listed by JBCPME, as discussed in the last section.

The X-ray data used in this work were obtained from the Proportional Counter Array (PCA; Jahoda et al (1996)) and the High Energy X-ray Timing Experiment (HEXTE; Rothschild et al. (1998)) aboard the RXTE observatory. The PCA consists of five proportional counter units (PCUs) operating in the 2 to 60 keV range, having a field of view of 1 degree in the sky( $^{\circ}$ ), and a time resolution of 1 micro second ( $\mu\text{sec}$ ) (see “The ABC of XTE” guide on the RXTE website<sup>2</sup>). The HEXTE instrument consists of two independent clusters of detectors. Each cluster contains four NaI(Tl)/CsI(Na) phoswich scintillation photon counters, and has a field of view of  $1^{\circ}$  in the sky. Effectively this instrument is sensitive to photons in the 15 to 240 keV range, and each photon’s arrival time accuracy is  $\approx 7.6 \mu\text{sec}$  (see “The ABC of XTE” guide). The first RXTE observation used in this work was obtained on 2005 November 18 (MJD 53692), and the last on 2007 April 23 (MJD 54213); the corresponding observation identification numbers (ObsID) are 91802-02-10-00 and 92802-01-21-00, respectively. This yielded 34 PCA timing residuals, but only 32 HEXTE residuals, since there were insufficient X-ray photons in the HEXTE data of ObsIDs 91802-02-12-00 and 92802-01-04-00. The PCA data was obtained in the event mode with identifier *E\_250us\_128M\_0\_1s*, after being integrated into time intervals of 244.14  $\mu\text{sec}$ , and binned in energy into 128 channels having non-uniform energy widths. In 20 ObsIDs useful data was available when all 5 PCUs were switched on; in 9 of them when only 4 PCUs were switched on; and so on. Even when only 1 PCU was switched on (ObsIDs 92802-02-06-00 and 92802-03-05-00) the data had sufficient number of photons to yield a statistically significant pulse profile.

---

<sup>2</sup>[heasarc.gsfc.nasa.gov/docs/xte/data\\_analysis.html](http://heasarc.gsfc.nasa.gov/docs/xte/data_analysis.html)

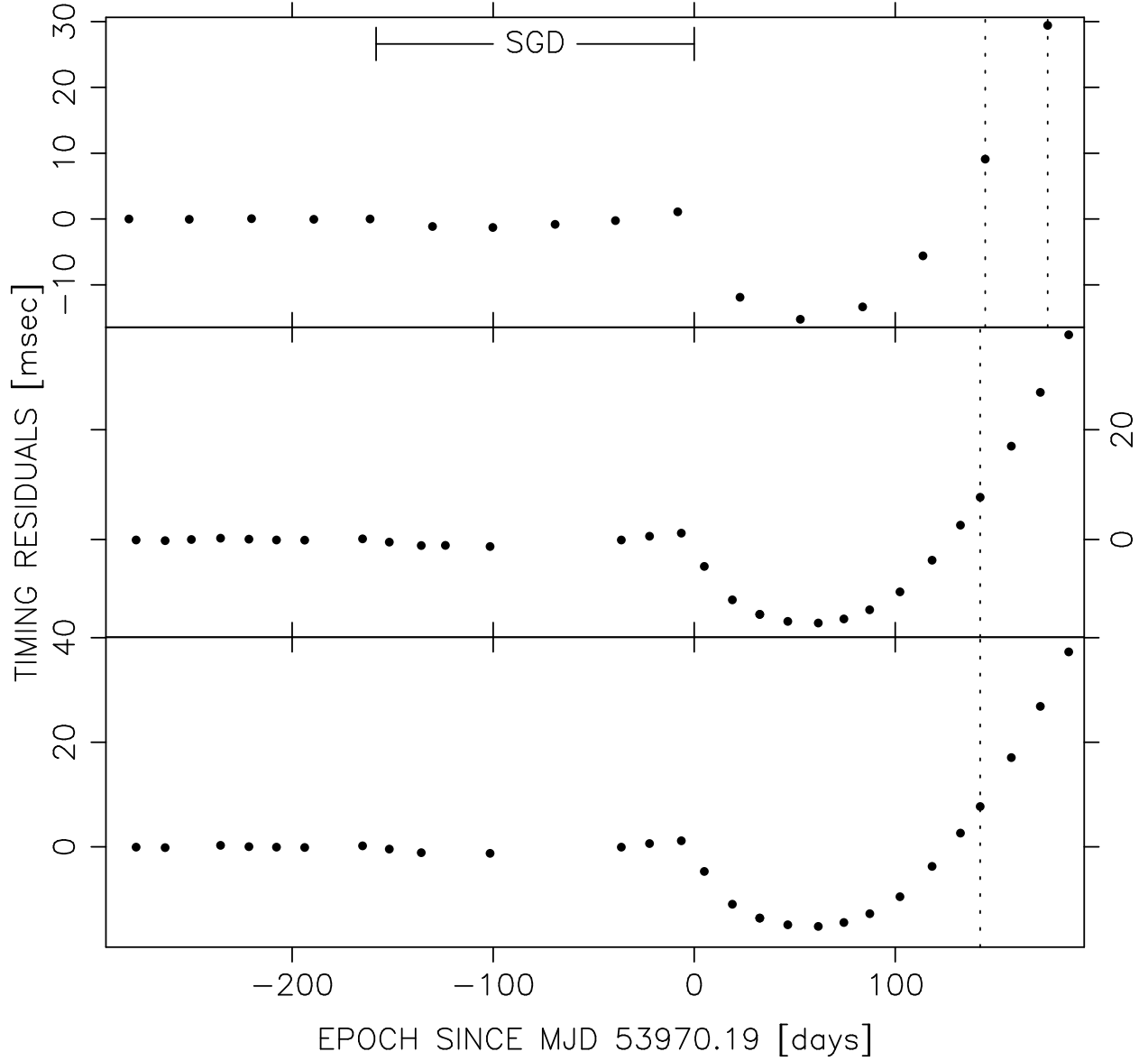


Fig. 1.— Timing residuals of the Crab Pulsar relative to the pre-glitch reference timing model given in Table 1. Residual 0 in each panel refers to the mean value of the residuals belonging to the pre-glitch duration of that panel. The dotted vertical lines are epochs after which a phase cycle of +1 had to be inserted into the timing data (using command PHASE +1 in TEMPO2). Data only up to MJD 54146 (day 175.81) has been shown to highlight the small depression extending from MJD  $\approx 53812.0$  (day  $\approx -158.19$ ) to day MJD 53970.19 (day 0.0); this has been marked as SGD in the figure. Top panel: Radio timing residuals from JBCPME. Middle panel: X-ray timing residuals from the RXTE/PCA data. Bottom panel: X-ray timing residuals from the RXTE/HEXTE data.

### 3. Analysis of Radio Data

The top panel of Figure 1 shows the radio timing residuals of the Crab Pulsar, relative to the pre-glitch reference timing model given in Table 1, during the epoch under consideration. The pre-glitch reference timing model was obtained using the first 5 data in the top panel of Figure 1, in the range MJD 53673.5 to MJD  $\approx 53812.0$ , translating to day  $-296.69$  to  $\approx -158.19$  in abscissa. This duration will henceforth be referred to as the pre-glitch duration (PGD). The TEMPO2 (Hobbs et al. 2006) best fit parameters of this data are shown in Table 1. The standard deviation of the five data, from the model derived by TEMPO2, is  $TRES = 38.6 \mu\text{sec}$ . However TEMPO2 estimates TRES using 5 degrees of freedom, whereas the number to use is 2, since 3 parameters have been fit for. The appropriate value of standard deviation is  $\sqrt{38.6^2 * 5/2} = 61 \mu\text{sec}$ .

By including the next five timing residuals in the top panel of Figure 1, from MJD  $\approx 53812.0$  to MJD 53970.19, or day  $\approx -158.19$  to 0.0 in abscissa, the TEMPO2 best fit parameters are  $\nu = 29.7749226293(8) \text{ Hz}$ ,  $\dot{\nu} = -372852.4(4) \times 10^{-15} \text{ s}^{-2}$ , and  $\ddot{\nu} = 1.14(1) \times 10^{-20} \text{ s}^{-3}$ . The TRES of these ten data is  $223.3 \mu\text{sec}$ , but the appropriate value of standard deviation is  $\sqrt{223.3^2 * 10/7} = 267 \mu\text{sec}$ . The two variances differ by  $267^2 - 61^2 = 67568$ , while the standard error on this difference is  $\sqrt{2 \times (267^4/7 + 61^4/2)} = 38287$ . The two variances differ by  $67568/38287 = 1.76$  standard errors; i.e., the latter variance is significantly larger than the former at the 92% confidence level. Attempts made to obtain statistical fits with standard deviation less than  $267 \mu\text{sec}$  failed (for example, by choosing a different reference epoch, by altering initial values of the parameters by hand, etc). Therefore using radio data right up to MJD 53970.19, to derive the pre-glitch reference timing model, is not justified. The reason is the small depression extending from MJD  $\approx 53812.0$  to MJD 53970.19 (day  $\approx -158.19$  to day 0.0) in the top panel of Figure 1, which will henceforth be referred to as the small glitch duration (SGD).

The main glitch that follows is clearly evident in the top panel of Figure 1. It starts at MJD 53970.19 and extends up to MJD 54250.5, or day 0.0 to 280.31 (henceforth referred to as the main glitch duration MGD), although data only up to MJD 54146 (day 175.81) has been shown in Figure 1 to highlight the depression.

Figure 2 shows a closer view of the top panel of Figure 1; earlier what looked like a depression now looks more like a glitch. Data points 3 to 7 in Figure 2 (five radio data points belonging to SGD) have been fit to the function  $f(t)$  in Equation 1, the fit taking into account their errors,

$$\begin{aligned} f(t) &= a_1(t - t_1) + \frac{b_1}{2}(t - t_1)^2 + \\ &\quad c_1 \left( 1 - \exp \left( \frac{-(t - t_1)}{\tau_1} \right) \right), \\ g(t) &= f(t_2) + a_2(t - t_2) + \frac{b_2}{2}(t - t_2)^2 + \\ &\quad c_2 \left( 1 - \exp \left( \frac{-(t - t_2)}{\tau_2} \right) \right), \end{aligned} \tag{1}$$

where the parameters  $t_{1,2}$  (epoch of the glitch),  $a_{1,2}$  (related to the permanent change in rotation frequency at the epoch of the glitch  $\Delta\nu_p$ ,  $b_{1,2}$  (related to the permanent change in rotation frequency derivative  $\Delta\dot{\nu}_p$ ,  $c_{1,2}$  (related to the exponential change in rotation frequency  $\Delta\nu_n$ ), and  $\tau_{1,2}$  (decay time scale of the glitch) are all allowed to vary during the non-linear fit (see Shemar & Lyne (1996) and Vivekanand (2015) for further details on Equation 1). Several equivalent fits are obtained by choosing the initial value of  $t_1$  between day  $-160$  and day  $-131$ , which is the range of epoch between the last data point of PGD and the first data point of SGD; the corresponding  $\tau_1$  obtained are 5.7 and 3.0 days respectively; larger values of  $t_1$  yield smaller values of  $\tau_1$ , as is expected. An illustrative fit, obtained using the initial value of  $t_1 = -146$  (midway between the above two numbers), is shown in the second row of Table 2. The corresponding  $f(t)$  is plotted as the dashed line in Figure 2. While the non-linear fit converged to the solution given with a standard deviation



Table 1: The pre-glitch reference timing model obtained using the first 5 data in the top panel of Figure 1, at reference epoch MJD 53750.0000002354282 (day  $-220.19$  in Figure 1).

The errors in the last digit of each number are shown in brackets.

Parameter	Value
Epoch (MJD)	53750.0000002354282
$\nu$ (Hz)	29.7749226271(1)
$\dot{\nu}$ ( $\text{s}^{-2}$ )	$-372853.5(4) \times 10^{-15}$
$\ddot{\nu}$ ( $\text{s}^{-3}$ )	$1.2(1) \times 10^{-20}$

Table 2: Results for the smaller glitch, derived from the best fit parameters, that are obtained by fitting  $f(t)$  to the data of the smaller glitch (SGD) in Figures 2 and 3 (data implies timing residuals in SGD, relative to the model of Table 1). In all three cases, the epoch of the glitch  $t_1$  is chosen or fixed as explained in the text. No error bars are shown for radio case since no degrees of freedom are left after the fit.

Data	$t_1$ (MJD)	$\Delta\nu_p$ ( $10^{-6}$ Hz)	$\Delta\dot{\nu}_p$ ( $10^{-13}$ $\text{s}^{-2}$ )	$\Delta\nu_n$ ( $10^{-6}$ Hz)	$\tau_d$ (days)
JBCPME	53824.2	0.005	$-0.018$	0.066	5.2
PCA	53811.9	$0.008 \pm 0.003$	$-0.019 \pm 0.004$	$0.03 \pm 0.03$	$8.3 \pm 6.7$
HEXTE	53811.9	$0.005 \pm 0.006$	$-0.015 \pm 0.006$	$0.03 \pm 0.04$	$15.7 \pm 12.4$

of 62  $\mu\text{sec}$ , fitting five data points to a function with five parameters leaves no degrees of freedom to estimate the errors on the parameters.

Attempts to fit the data to a modified  $f(t)$ , that does not contain the last ( $c_1$  and  $\tau_1$ ) term, converge to values of  $t_1$  lower than the epoch of the last data point of PGD. These are unrealistic solutions, since the first residual after a glitch must have more negative value than that of the pre-glitch reference timing model. This shows that inclusion of the decay time is critical in the fit, further supporting the assertion that what looks like a small depression is probably a small glitch, although timing noise can not be ruled out. However, one must keep in mind that the function  $f(t)$  has five parameters, and only five data are used in the fit in this section. While it is true that a set of 5 data points can not be fit to any arbitrary function of 5 parameters, particularly if the function is a mixture of polynomials and exponential, one must be open to the possibility that the data of SGD may also be due to timing noise.

Next, the radio data belonging to MGD are fit to the function  $g(t)$  of Equation 1. Ideally this should be done after subtracting  $f(t)$  from the timing residuals of MGD. Here it is assumed that  $f(t)$  is much smaller than  $g(t)$  for the MGD epochs; so  $g(t)$  is fit to the residuals without subtracting  $f(t)$ , since the derived glitch parameters are not expected to be statistically rigorous anyway. It has been verified that results of both approaches are statistically consistent. A fit varying all parameters converges to the unrealistic situation of  $t_2$  being less than the epoch of the last data of SGD. By fixing  $t_1$  at various epochs between that of last data point of SGD and that of the first data point of MGD (non inclusive), various solutions can be obtained in which  $\tau_2$  varies consistently. Solutions closer to the former data point appear to have lower standard deviation. The solution shown in the second row of Table 3 is an illustrative one, where  $t_2$  has been fixed to a value mid way between the above two points, while the rest of the four parameters have been varied.

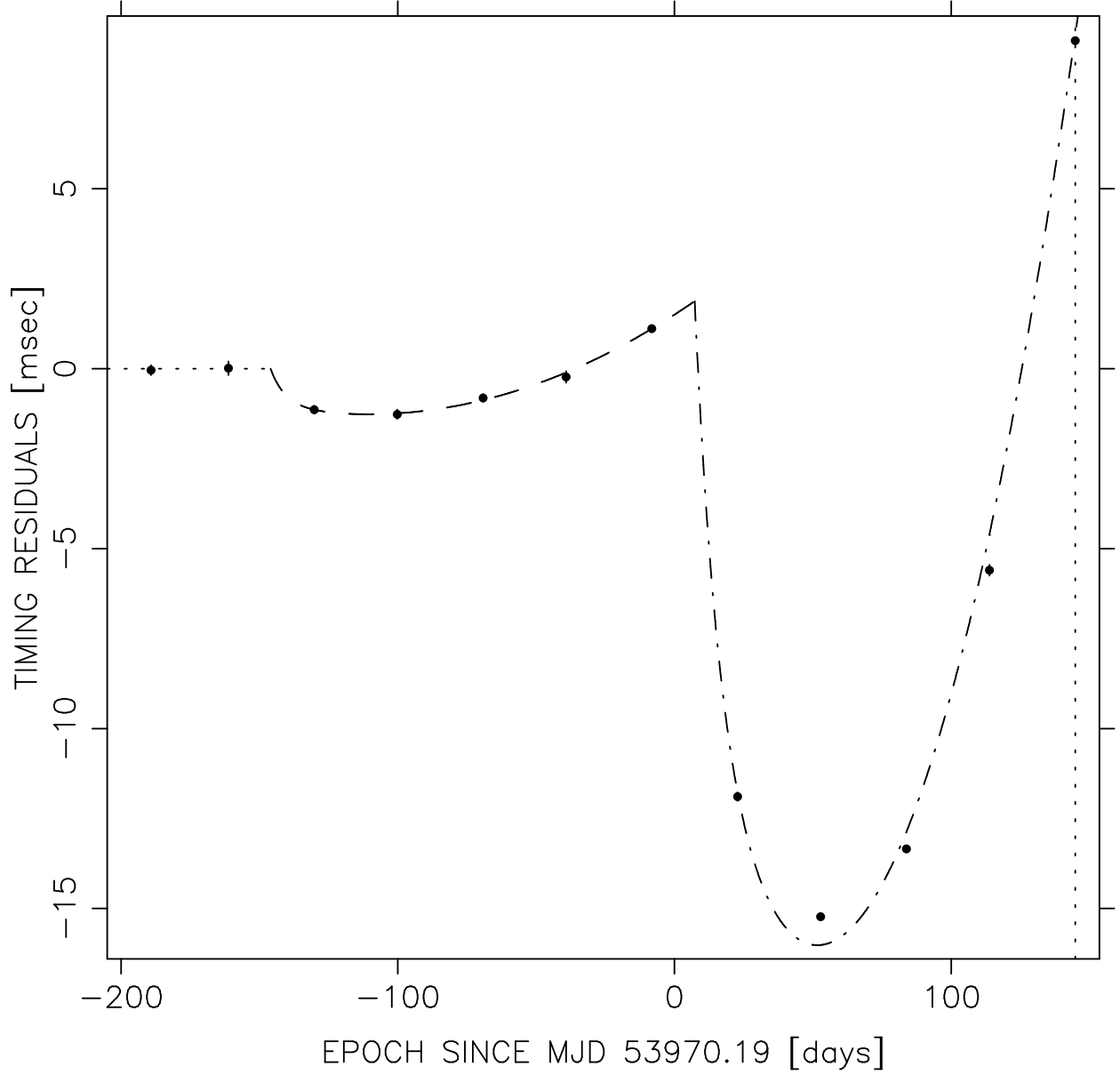


Fig. 2.— A closer look at the top panel of Figure 1, from MJD 53765.19 to MJD 54120.19 (days  $-205$  to  $+150$  in the figure). The dashed line is the function  $f(t)$ , defined in Equation 1, with the parameters given in the second row of Table 2. The dashed-dotted line is the function  $g(t)$  with the parameters given in the second row of Table 3. The horizontal dotted line represents the pre-glitch reference timing model of Table 1.

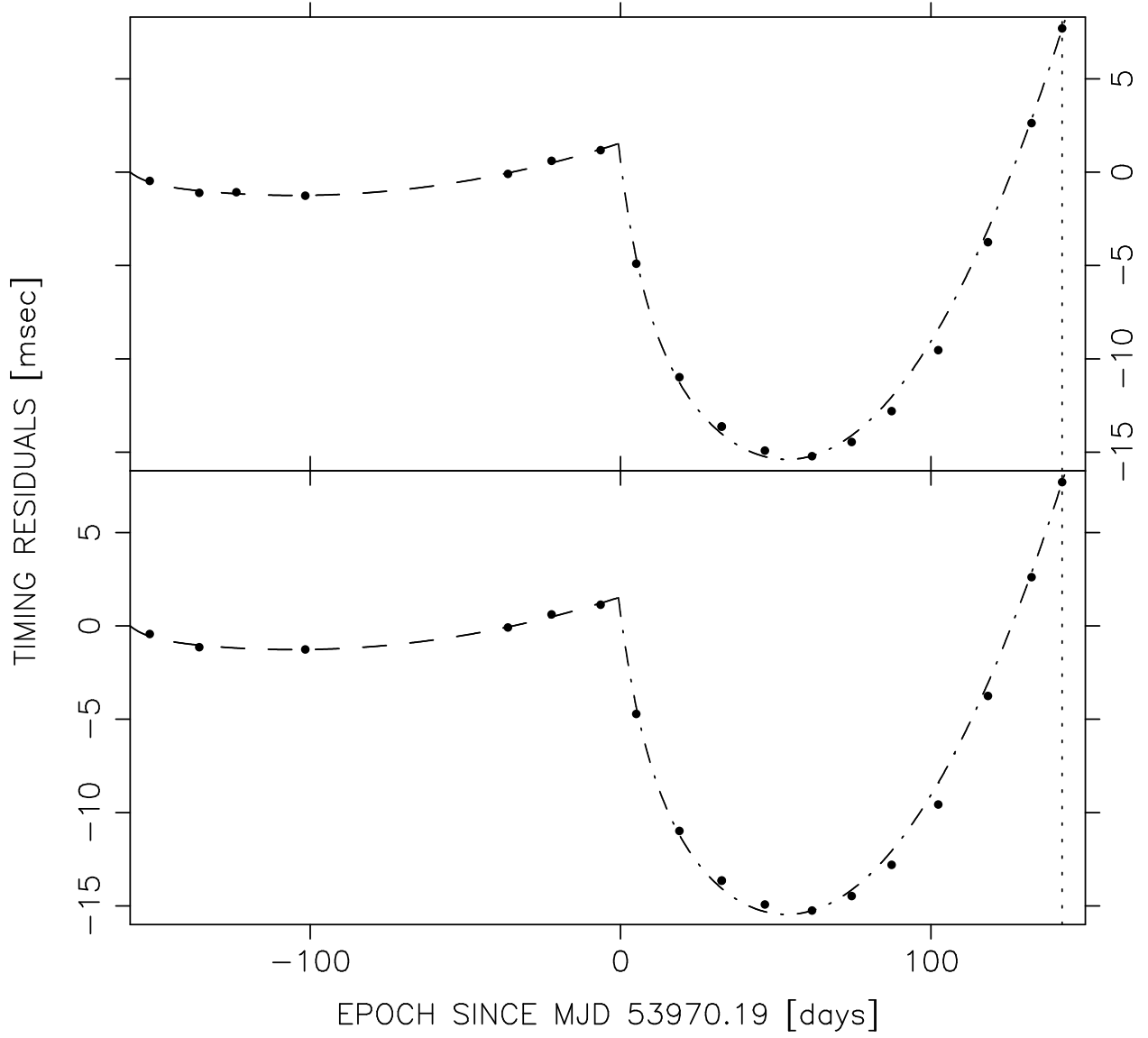


Fig. 3.— Top Panel: A closer look at the middle panel of Figure 1, from MJD 53824.19 to MJD 54120.19 (days  $-146$  to  $+150$  in the figure). The dashed line is the function  $f(t)$  with the parameters given in the third row of Table 2. The dashed-dotted line is the function  $g(t)$  with the parameters given in the third row of Table 3. Bottom Panel: A closer look at the bottom panel of Figure 1, from MJD 53824.19 to MJD 54120.19 (days  $-146$  to  $+150$  in the figure). The dashed line is the function  $f(t)$  with the parameters given in the bottom row of Table 2. The dashed-dotted line is the function  $g(t)$  with the parameters given in the bottom row of Table 3.

The corresponding curve is the dashed-dotted curve in Figure 2. Although the parameters in the second row of Table 3 are consistent with the results derived by both JBO and XAO for CPG2006, the radio data used in this work are not suitable to derive rigorous glitch parameters. It is therefore concluded that the CPG2006 event was preceded by a small glitch. However, it should be kept in mind that this result depends critically upon the pre-glitch reference timing model derived above, for which unfortunately only 5 radio timing residuals were available. Therefore the result of this section do not rule out timing noise altogether.

#### 4. Analysis of X-Ray Data

The results derived using radio data are now verified using X-ray data from the RXTE observatory. Vivekanand (2015) and Vivekanand (2016) discuss in detail the analysis of Crab Pulsar data from the HEXTE and PCA instruments, respectively. In this work one has to additionally filter the PCA data for time markers, using the tool *fselect* along with a bitfile containing the script “Event == b1xxxxxxxxxxxxxxxxx” (see “The ABC of XTE” guide), because of the data mode of PCA. The same must be done when using the tool *seextrct* to obtain the light curve.

TEMPO2 fits to the 8 PCA residuals and the 7 HEXTE residuals in the PGD (see the middle and bottom panels of Figure 1), resulted in pre-glitch reference timing models that had standard deviation of data TRES of 111  $\mu\text{sec}$  and 114  $\mu\text{sec}$ , respectively. After taking into account the true degrees of freedom, the above two standard deviations become 140  $\mu\text{sec}$  and 151  $\mu\text{sec}$  respectively. By including the SGD data also, the TEMPO2 fits yield pre-glitch reference timing models with corrected standard deviations of 231  $\mu\text{sec}$  and 268  $\mu\text{sec}$  respectively. By the argument of the previous section both sets of variances (231, 140 and 268, 151) differ at the 82% confidence level. Therefore both the PCA and the HEXTE

data confirm the result of the previous section, that one is not justified in including the SGD data to obtain the pre-glitch reference timing model for CPG2006.

Although the glitch behavior in the X-ray data of SGD is evident when these timing models are used, they are clearly worse than the pre-glitch reference timing model obtained from the radio data. Therefore the latter has been used to analyze the X-ray data.

The top panel of Figure 3 shows a closer view of the middle panel of Figure 1. Fitting the function  $f(t)$  to the 7 PCA data in the SGD does not converge to a solution if all five parameters are varied, for several initial values of  $t_1$  and  $\tau_1$ . Therefore for illustrative purposes  $t_1$  was fixed midway between the last PCA data point of PGD and the first PCA data point of SGD. The corresponding  $f(t)$  is plotted as the dashed line in the top panel of Figure 3, while the corresponding parameters, or the results derived from them, are listed in the third row of Table 2; the standard deviation of the data from this solution is  $76 \mu\text{sec}$ . Attempts to fit the function  $g(t)$  to the 19 PCA data of MGD by varying all five parameters either resulted in unrealistic solutions of  $t_1$ , or did not converge to a solution. Therefore for illustrative purposes  $t_1$  was fixed midway between the last PCA data point of SGD and the first PCA data point of MGD. The corresponding  $g(t)$  is plotted as the dashed-dotted line in the top panel of Figure 3, while the corresponding parameters, or the results derived from them, are listed in the third row of Table 3.

The bottom panel of Figure 3 shows a closer view of the bottom panel of Figure 1. Fitting the function  $f(t)$  to the 6 HEXTE data in the SGD by varying all parameters led to results similar to those in the PCA case. Therefore for illustrative purposes  $t_1$  was fixed midway between the last HEXTE data point of PGD and the first HEXTE data point of SGD. The corresponding  $f(t)$  is plotted as the dashed line in the bottom panel of Figure 3, while the corresponding parameters, or the results derived from them, are listed in the last row of Table 2; the standard deviation of the data from this solution is 57

$\mu\text{sec}$ . Attempts to fit the function  $g(t)$  to the 19 HEXTE data of MGD by varying all five parameters resulted in unrealistic solutions of  $t_1$ . Therefore for illustrative purposes  $t_1$  was fixed midway between the last HEXTE data point of SGD and the first HEXTE data point of MGD. The corresponding  $g(t)$  is plotted as the dashed-dotted line in the bottom panel of Figure 3, while the corresponding parameters, or the results derived from them, are listed in the last row of Table 3.

The behavior of the fits to X-ray data in Figure 3 is very similar to that in Figure 2. It is therefore concluded that the X-ray data confirm the results obtained from radio data.

## 5. Discussion

It is clear from the analysis of the monthly radio data (Figure 2, Table 2 and the analysis of section 3) that the Crab Pulsar most probably suffered a small glitch before CPG2006. This is verified by the X-ray data (Figure 3, Table 2 and the analysis of section 4).

As already mentioned, the data available for this work is quite sufficient to demonstrate the existence of something that looks like a small glitch, but not to derive rigorous glitch parameters. So the parameters used to plot the functions  $f(t)$  and  $g(t)$  in Figures 2 and 3 (listed in Tables 2 and 3) should be taken as illustrative. Even then, the values of  $\tau_2$  in Table 3 are consistent with the values  $7.3 \pm 0.3$  days derived by Wang et al. (2012). The value of  $\Delta\nu_p + \Delta\nu_n$  in the second row of Table 3 is  $0.58 \pm 0.20$  micro Hertz, which is consistent with the value of  $0.41 \pm 0.09$  derived by Wang et al. (2012). The ratio of change in rotation frequency  $(\Delta\nu_p + \Delta\nu_n)/\nu \times 10^9$  from the second row of Table 3 is  $19 \pm 7$ , which is consistent with the value  $21.8 \pm 0.2$  derived by Espinoza et al. (2011). The ratio of change in rotation frequency derivative  $(\Delta\dot{\nu}_p + \Delta\dot{\nu}_n)/\dot{\nu} \times 10^3$  from the second column of Table 3

is  $1.8 \pm 0.7$ , which is roughly consistent with the value  $3.1 \pm 0.1$  derived by Espinoza et al. (2011), and the value 1.3 estimated from Wang et al. (2012). Thus the illustrative radio solution in the second row of Table 3 is consistent with earlier estimates; this is expected since the small glitch perturbs only weakly the pre-glitch reference timing model for the main glitch. The X-ray solutions in the last two rows of Table 3 are consistent with this radio solution. This can also be taken as indirect validation of the illustrative radio solution for the small glitch in Table 2, since this is used to derive the solution for the main glitch. The X-ray solutions in the last two rows of Table 2 are consistent with the radio solution for the small glitch (second row of Table 2), as expected.

The small glitch is also evident in the  $\nu$  and  $\dot{\nu}$  data of JBCPME. By fitting a straight line to the five  $\dot{\nu}$  data of the PGD, it is seen that the next five  $\dot{\nu}$  (belonging to the SGD) lie systematically lower (larger in magnitude) than the line, by at least  $-18(\pm 7) \times 10^{-15} \text{ s}^{-2}$ , which is the typical signature of a very small glitch in the Crab Pulsar. By doing the same with the  $\nu$  data, it is seen that  $\nu$  increases systematically in the SGD. Although one expects such an increase to be sudden just after a glitch, this result also indicates that the  $\nu$  and  $\dot{\nu}$  of the Crab Pulsar had probably behaved similar to those during a glitch in the boundary region between PGD and SGD.

The PGD in the radio data apparently can not be extended to lower epochs; the residuals for the epochs MJD 53658 and MJD 53628 lie systematically above those of the five PGD residuals. This is also apparent in the  $\dot{\nu}$  data of JBCPME, which are more positive before the PGD.

Did the glitch detector of Espinoza et al. (2014) detect this small glitch? It probably did, and probably classified it as one of their 381 Glitch Candidates (GC). Espinoza et al. (2014) allow for the possibility that some of the GC might be real glitches, but believe most of them are due to timing noise. Therefore it is likely that Espinoza et al. (2014) believe



that this event is not a glitch but is on account of timing noise. The fact, that the  $c_1$  and  $\tau_1$  term in  $f(t)$  (in Equation 1) is required to give a sensible fit to the SGD data, gives some support for the belief that one is dealing with a glitch and not timing noise. On the other hand, Espinoza et al. (2014) may have missed this glitch, due to their methodology. They use 20 times of arrival (TOA) to obtain the pre-glitch reference timing model, and fit a quadratic function to the next 10 TOA. It is possible that these numbers are inadequate for sensing the small glitch of this work. Furthermore, they were looking for a sudden rise in rotation frequency  $\nu$ , whereas, as indicated by the  $\nu$  data of JBCPME, this may be a slower glitch. In this context, this work focuses attention on the problem of distinguishing between a small glitch and timing noise in pulsars.

It appears unlikely that the small glitch and CPG2006 are causally connected, since they are separated by about  $\approx 150$  days. There are glitches in the Crab Pulsar separated by much smaller time – the glitches of MJD 50459 and MJD 50489 are separated by a mere 30 days, although there is doubt whether the latter is a glitch at all (Wong et al. 2001).

As Espinoza et al. (2014) point out, although the exact mechanism for glitches is not fully understood, the glitch magnitude distribution in general, and the magnitude of the smallest glitch in particular, in the Crab Pulsar, is an important information. The magnitude of a glitch is related to the number of super fluid vortices that unpin during the event (see Alpar et al. (1996) and Ruderman et al. (1998)). Clearly the smallest glitch in a pulsar will set constraints on the minimum size of the region in the inner crust that is involved in the glitch process. The numbers derived in the second row of Table 2 are not reliable enough to estimate rigorously the magnitude of the small glitch. This is best done using the daily sampled data of the JBO. The higher the dynamic range of glitch magnitudes (the ratio of the maximum to the minimum observed glitch magnitude) in the Crab Pulsar, the better one can derive the distribution of glitch magnitudes; some

theoretical models predict a power law distribution (Warszawski & Melatos 2008).

The size of a glitch depends upon the number of unpinned vortices, the details of pinning and repinning of these vortices, and the location of unpining (Warszawski & Melatos 2011). In particular the size of a glitch depends upon the pinning strength, stronger pinning causing larger glitches, although Warszawski & Melatos (2011) point out that this belief is not very obvious – contrary behavior is also possible. Therefore the smallest possible glitch in a pulsar may set constraints on the distribution of pinning strengths in the crust, at the lower end of the distribution. The smallest possible glitch in a pulsar may also suggest that the crust is lighter rather than heavier (Warszawski & Melatos 2011), which may have implications for the equation of state of a neutron star.

In summary, this work demonstrates a peculiar behavior of the timing residuals of the Crab Pulsar that started around late March/early April 2006, and continued up to the epoch of the main glitch. This work has shown that this behavior is consistent with that of a small glitch. If this is true, then this is probably the smallest glitch detected so far in the Crab Pulsar, whose implications have been discussed above. On the other hand this work does not rule out timing noise. Therefore, future pulsar timing programs will need not only better sensitivity but also fast cadences in order to be able to study the small glitches regime. If it turns out that this is indeed timing noise, then there are far reaching implications for the definition of timing noise. The current consensus is that timing noise is supposed to be that which is left over in timing residuals after the effects of secular variations and glitches have been removed (Lyne et al. (1993)). Clearly the understanding of the term timing noise needs to be revised if it starts behaving like small glitch.

I thank the referee Cristóbal Espinoza for detailed and helpful comments. This research made use of data obtained from the High Energy Astrophysics Science Archive Research Center Online Service, provided by the NASA-Goddard Space Flight Center.

Table 3: Results for the larger glitch, derived from the best fit parameters, obtained by fitting  $g(t)$  to the data of the main glitch (MGD) in Figures 2 and 3 (data implies timing residuals in MGD, relative to the model of Table 1). In all three cases, the epoch of the glitch  $t_2$  has been fixed mid way between the last data point of SGD and the first data point MGD.

Data	$t_1$ (MJD)	$\Delta\nu_p$ ( $10^{-6}$ Hz)	$\Delta\dot{\nu}_p$ ( $10^{-13}$ s $^{-2}$ )	$\Delta\nu_n$ ( $10^{-6}$ Hz)	$\tau_d$ (days)
JBCPME	53977.5	$0.083 \pm 0.007$	$-0.223 \pm 0.004$	$0.5 \pm 0.2$	$8.9 \pm 2.7$
PCA	53969.5	$0.110 \pm 0.004$	$-0.233 \pm 0.005$	$0.4 \pm 0.1$	$7.8 \pm 2.1$
HEXTE	53969.5	$0.108 \pm 0.004$	$-0.232 \pm 0.005$	$0.3 \pm 0.1$	$8.9 \pm 2.4$

## REFERENCES

- Alpar M. A., Chau H. F., Cheng K. S., Pines D., 1993, ApJ, 459, 706
- Baym G., Pethick C., Pines D., Ruderman M., 1969, Nature, 224, 872
- Espinoza, C. M., Lyne, A. G., Stappers, B. W., and Kramer, M. 2011, MNRAS, 414, 1679
- Espinoza, C. M., Antonopoulou, D., Stappers, B. W., Watts, A. and Lyne, A. G. 2014, MNRAS, 440, 2755
- Haskell, B. and Melatos, A. 2015, International Journal of Modern Physics D, Vol. 24, No. 3, 1530008
- Hobbs, G. B., Edwards, R.T. and Manchester, R. N. 2006, MNRAS, 369, 655
- Jahoda, K., Swank, J. H., Giles, A. B. et al 1996, Proc. SPIE, 2808, 59
- Lyne, A. G., Pritchard, R. S. and Graham Smith, F. 1988, MNRAS, 233, 667
- Lyne, A. G., Pritchard, R. S. and Graham Smith, F. 1993, MNRAS, 265, 1003
- Lyne, A. G., Shemar, S. L., and Graham Smith, F. 2000, MNRAS, 315, 534
- Lyne, A. G., Jordan, C. A., Graham Smith, F. et al 2015, MNRAS, 446, 857
- Rothschild, R. E., Blanco, P. R., Gruber, D. E., Heindel, W. A., MacDonald, D. R., Marsden, D. C., Pelling, M. R. and Wayne, L. R. 1998, ApJ, 496, 538
- Ruderman, M., Zhu, T. and Chen, K. 1998, ApJ, 492, 267
- Shemar, S. L. and Lyne, A. G. 1996, MNRAS, 282, 677
- Vivekanand, M. 2015, ApJ, 806, 190
- Vivekanand, M. 2016, A&A, 586, A53

Wang, J., Wang, N., Tong, H., Yuan, J. 2012, Ap&SS, 340, 307

Wong, T., Backer, D. C. and Lyne, A. G. 2001, ApJ, 548, 447

Warszawski L., Melatos A. 2008, MNRAS, 390, 175

Warszawski L., Melatos A. 2011, MNRAS, 415, 1611